2016 American Control Conference (ACC)
Boston Marriott Copley Place
July 6-8, 2016. Boston, MA, USA

# Optimal Mode-Switching and Control Synthesis for Floating Offshore Wind Turbines

Behrooz Shahsavari[1,2], Omid Bagherieh[1], Negar Mehr[1], Roberto Horowitz[1] and Claire Tomlin[2]

*Abstract*— **This paper proposes a multi–objective optimal control and switching strategy for floating offshore wind turbines when the wind speed can be approximately predicted. The system is modeled as a hybrid automaton with two modes corresponding to the turbine operation in low– and high–speed wind profiles. The main control objective in the low–speed wind mode is to maximize the total captured power in a finite time horizon, whereas in the high–speed mode, it is desired to regulate the generator torque and speed around predefined rated values even under gust loads. The problem is formulated as a constrained mixed–integer bilinear program in a model predictive control framework. The posed constraints correspond to the electrical/mechanical limitations of the blade actuators and generators. Various practical considerations, such as minimizing the number of switching occurrences and mechanical fatigue prevention, are explicitly considered in the optimization problem. The proposed control method is applied to the dynamical model of a real wind turbine and simulation results are presented.**

## I. Introduction

Wind as a source of renewable energy has attracted the attention of many researchers in recent years because of its cleanness and sustainability [1]. Although the term *wind turbine* usually reminds people of hills where a large number of wind turbines are installed, offshore wind turbines are in fact the preeminent machines for capturing wind energy. This is due to the higher wind speed at seas, vast available area for turbine installation, and more stable speed of wind above seas. Moreover, the noise generated by wind turbines is much more tolerable in offshore wind farms, and visual impact is less obtrusive.

Offshore platforms add to the difficulty of controller design for wind turbines [2]–[7] since the platform is unactuated, and the effect of its movement on energy harvesting must be compensated through controlling the blade angles. Minimizing the overall cost of wind energy harvesting is crucial in order for offshore wind turbines to be capable of competing with fossil fuel energy in the energy market. Such a decrease in costs incurred by wind turbines can be achieved by increasing the efficiency and lifetime of wind turbines as well as reducing maintenance costs. One of the most economical ways for decreasing power generation costs is using feedback/feedforward control without adding significant hardware or modification to the structure. Several objectives for a controller can be defined among which, increasing energy capture efficiency in low wind speed regime and regulating the energy capture in high wind speed regime (while not violating the actuators and power limitations of the turbine) are the paramount ones. As division of the desired objectives into the above two categories suggests, there exists a switching between low and high wind speed operating modes of a wind turbine. In [2], [8], [9] a pre-determined switching point between low and high speed regimes has been considered. In contrast to using predetermined operation regimes and fixed control laws, this study aims to find the *optimal* low and high speed regimes of wind turbines and their corresponding control rules such that maximum energy capture is achieved with minimum platform pitch movement.

Model Predictive Control (MPC) is widely known as one of the most desirable control schemes as it enables the control engineer to impose objectives and also constraints of interest directly in an optimization problem that has to be solved at every time step [10]. This framework is very suitable for smart power control problems [11] such as the topic of this study because there are various operational constraints enforced by the turbine actuators and generator, which should not be ignored in the control design. For instance, the blades movements/speeds are limited, and generator speed should not exceed a maximum allowed value.

In order to implement a model predictive controller, it is crucial to obtain an accurate dynamical model of the system. Various models have been proposed by researchers for this purpose. In [12], neural networks are trained on an existing set of data for obtaining a model for the highly non–linear dynamics of a wind turbine and prediction of wind speed. Detailed models particularly for floating offshore wind turbines are considered in several articles [2]–[4], [13], which mostly use a software called *FAST* (Fatigue, Aerodynamics, Structures, and Turbulences) [14] developed at the National Renewable Energy Laboratory (NREL), U.S.A. In this work, FAST is utilized for the task of modeling the wind turbine.

Non–linear dynamics of wind turbines is taken into account in [15] by implementing a scheduled model predictive controller for high wind speed operation in which regulating the generator speed is the main objective. Several linear models of turbines are used in a model predictive control fashion, and the final control input is a weighted sum of control inputs obtained for each linear model. In [16], model predictive control is used for regulating power in a wind farm satisfying battery storage restrictions. In [17], it is shown that taking advantage of wind speed measurement and prediction

[1]Department of Mechanial Engineering, University of California, Berkeley, CA 94720, USA.

[2]Department of Electrical Engineering and Computer Sciences, University of California, Berkeley, CA 94720, USA. {behrooz, omidba, negar.mehr, horowitz}@berkeley.edu tomlin@eecs.berkeley.edu

techniques such as LIDAR (LIght Detection and Ranging) in a non–linear model predictive control yields to a significant increase in efficiency.

Similar to the stated literature, our proposed control design benefits from knowing a rough estimate of the upstream wind speed which, in practice, can be obtained by LIDAR technology [18]. The information provided by such sensors is used in order to obtain an optimal control using model predictive control strategy. Despite previous work where MPC was applied to wind turbines mounted on fixed platforms[18]–[20], in this work, we consider MPC for floating platform turbines. This is an important distinction and requires a different type of control strategy since platform movement changes the relative angle/speed between the wind and blades, yielding to significant energy loss if not compensated. Despite the prior MPC studies on offshore wind turbines [21], our proposed method does not consider a fixed switching point and does not ignore the fact that the relative speed between the wind and blades plays a crucial role in determining the energy capture and switching point. We consider three main factors, namely maximizing the energy capture, minimizing platform movement and number of switching occurrences to prevent structural fatigue in defining the optimization value function. On the other hand, we pose a set of constraints to explicitly take the blade pitch angle/speed limitations and generator maximum output power into account. Subject to these constraints, the switching points in conjunction with the control rules for low and high wind speed regimes are optimally determined.

The rest of this paper is organized as follows. In section II, the underlying nonlinear dynamics governing offshore wind turbines, and a simplified linearized model for that are discussed briefly. It is followed by introducing wind turbine operating modes and their special characteristics in section III. In section IV, the control problem objectives and constraints are described, and the problem is formalized in a hybrid MPC framework. The results of a simulation study for different scenarios are illustrated in section V, and conclusions are drawn in section VI.

## II. Wind Turbine Model

An accurate plant model is a crucial requirement of model–based control design. In [2], *Jonkman et al.* have obtained an accurate nonlinear model of a floating offshore wind turbine and have implemented it in software *FAST* [14]. As a running example, we use *FAST* to obtain a simplified model of a specific floating offshore horizontal–axis wind turbine (*NREL 5.0 MW Baseline Wind Turbine* [14]) with the following state vector $x$, control input $u$, and (sampled) disturbance $d$

$$\begin{aligned} x =: &[p \text{ (platform pitch angle)}, \ \dot{p}, \ \omega_r \text{ (rotor speed)}]^T \\ u =: &[T_g \text{ (generator torque)}, \ \beta \text{ (blade pitch angle)}]^T \\ d =: &[v \text{ (wind speed)}]. \end{aligned} \tag{1}$$

The interested reader can refer to [4], [5] for more details about these system parameters. We linearize the original model by following the procedure given in [4], [6], where the model was linearized around wind speed of $18m/s$. Besides the above states, we assume that feedback is available from three other variables, namely the rotor speed, wind speed and (estimate) of upstream wind speed.

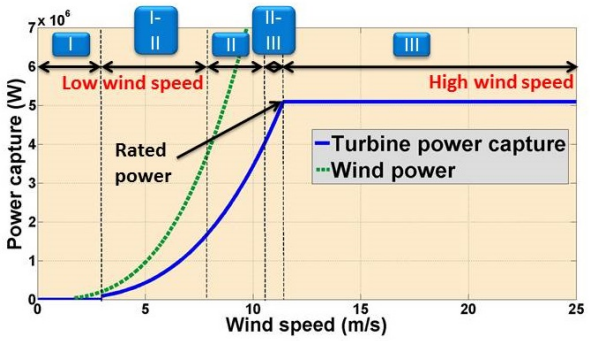


Fig. 1: The operating region of a wind turbine.

## III. Wind Turbine Operating Regions

Figure 1 illustrates distinct operation modes of a wind turbine distinguished based on the wind speed. The green dotted and blue solid curves show the available energy in the wind and the energy which can be captured by the turbine, respectively. As Fig. 1 displays, wind turbine operating regions are divided into three main categories, denoted by I, II and III as well as transition regions between them.

In region I, $R_1$, the wind speed is not big enough to turn on the turbine. In region II, $R_2$, the turbine is operating in low wind speed, and energy capture increases by increase in wind speed. In region III, $R_3$, the generator can not capture more than rated power of the turbine which is 5 MW in this figure. Therefore, power capture is regulated to 5 MW in $R_3$. There are transition regions between $R_1$ and $R_2$ as well as $R_2$ and $R_3$. In this work, we focus on transition between $R_2$ and $R_3$ as well as optimal control in these two regions.

The low wind speed operating region, $R_2$, and high wind speed operating region, $R_3$, for the specific turbine considered here are respectively given by

$$v_{R_2} := \{v : 7.8 \leq v \leq 10.5\}, \quad v_{R_3} := \{v : 11.4 \leq v \leq 25\}.$$

where $v(m/s)$ denotes the wind speed. In $R_2$, generator torque is the only actuator used to maximize power capture. On the other hand, in $R_3$, blade pitch angle is utilized to regulate power capture to the rated power, and generator torque is kept constant. The switching strategies used in the literature consider a specific wind speed for switching between these two regions and only utilize generator torque as the control input. In this work, our goal is to maximize efficiency while transitioning between these two regions. Therefore, a switching point is obtained online based on the prediction of wind speed and current operating condition of the system. Also, both generator torque and blade pitch angle are used as control inputs.

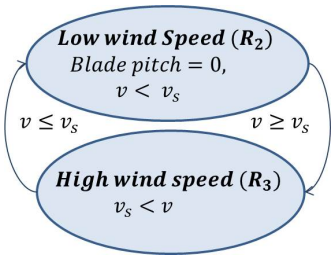


Fig. 2: A hybrid automaton of a floating offshore wind turbine system.

## IV. Control Design

Since the sequence of modes in our application is fixed and known due to *a priori* knowledge (Fig. 2), in this work, we aim to find an optimal switching strategy for a given switching sequence – as in Fig. 2 – along with optimal control for nodes $R_2$ and $R_3$. We define a formal mathematical representation of the optimization problem that was intuitively described in the previous sections. The key idea is that we take the advantage of having an *a priori* knowledge about the wind in a finite horizon of the future, which is usually measured/predicted by weather observing equipment – e.g. a radar or a Sonic Detection And Ranging (SODAR) meteorological instrument, making receding horizon control an appropriate candidate for synthesizing control.

We formulate the problem in a hybrid model predictive control (HMPC) framework with an objective to maximize the captured electrical power while the platform pitch angle and switching occurrences are kept small, and the constraints arising from mechanical limitations of the actuators are satisfied . In the sequel, we will formalize these optimization objectives and constraints.

### A. Optimization Objective

*1) Power:* The main control objective is to maximize the electrical power captured from wind. Denote $P_g^k$ as the HMPC objective function at time step $k$, which is equal to the generator power summed over the HMPC horizon, say $H$, excluding the last step

$$J^k = P_g^k = \sum_{i=k}^{k+H-2} T_g(i)\omega_g(i). \tag{2}$$

where, $T_g(i)$ and $\omega_g(i)$ refer to the generator torque and rotational speed at time step $i$ respectively.

*2) Platform Pitch Angle:* Due to mechanical fatigue caused by variations of platform pitch angle, we consider a penalized value function in order to take both the power and platform pitch angle into account.

$$J^k = \sum_{i=k}^{k+H-2} T_g(i)\omega_g(i) - \lambda_1 \sum_{i=k}^{k+H-1} |p_i|$$

Here $p_i$ denotes the platform pitch at time step $i$ and $\lambda_1 \geq 0$ is a penalty weighting parameter chosen by the designer.

*3) Switching Occurrences:* As number of switching is correlated with the fatigue in the blades, we further penalize the value function with the number of switching occurrences in the HMPC horizon

$$\begin{aligned} J^k = &\sum_{i=k}^{k+H-2} T_g(i)\omega_g(i) - \lambda_1 \sum_{i=k}^{k+H-1} |p_i| \\ &- \lambda_2 \sum_{i=k}^{k+H-2} |\gamma(i+1) - \gamma(i)| \end{aligned} \tag{3}$$

where $\gamma$ is a binary variable encoding by the current operating region,

$$\gamma(i) := \begin{cases} 1 & \text{if } q(i) \in R_3 \\ 0 & \text{if } q(i) \in R_2 \end{cases}, \tag{4}$$

where $q(i)$ is the discrete state of the system at time step $i$.

### B. Constraints

The constraints are divided into two types: constraints on the continuous variables (e.g. states or inputs), and logic implications that determine the discrete states of the system.

*1) System dynamics:* Throughout this paper, we focus on the dynamics from three inputs, namely the generator torque, blade pitch (control inputs) and wind speed (disturbance input), to three continuous states which are the platform pitch angle, platform pitch rate and generator speed. The nonlinear dynamics as well as linearized dynamics are explained in Section II. This linearized model is discretized using sampling time of 0.5 second which is reasonable for wind speed variation.

*2) Transition relation:* Finding optimal switching strategy based on wind prediction is in contrast with most of the other works specifying fixed wind speeds as the switching thresholds between the "low wind speed" and "high wind speed" regimes. We define an adaptive transition relation by

$$\begin{aligned} q(i) = R_3 \Leftrightarrow V(i) \geq V_s^k, \quad & k \leq i \leq k+H-1 \\ q(i) \in \{R_2, R_3\}, \quad & i \geq 0 \end{aligned} \tag{5}$$

where $V_s^i$ is the switching wind speed defined by the HMPC at time step $i$. Note that this constraint along with the bilinear objective function makes our problem a *mixed-integer bilinear program.*

*3) Generator torque:* The generator torque is subjected to lower and upper bound constraints incurred electro-mechanical limitations:

$$T_g^{lb} \leq T_g(k) \leq T_g^{ub} \tag{6}$$

It is worth noting that even if these constraints do not really exist, considering an upper and lower bounds for the generator torque as an optimization variable can result in a faster convergence in some optimization algorithms. Torque variation rate is also subjected to an upper limit captured by $\dot{T}_g(t) \leq \dot{T}_g^{max}$ in continuous time, and approximated in discrete time by

$$\begin{aligned} |T_g(k+1) - T_g(k)| &\leq \delta_{T_g} \\ \delta_{T_g} &= \dot{T}_g^{max} \times \tau \end{aligned} \tag{7}$$

where $\tau$ is the sampling time of the controller.

The last constraint corresponding to torque regulation in high wind speed region, $R3$, can be either considered as a penalized optimization objective or a hard constraint. Suppose $T_g^\circ$ is the desired *rated torque* associated with the *rated power* shown in Fig. 1. The former approach can be pursued by adding the following term to the value function

$$-\lambda \sum_{i=k}^{k+H-1} \gamma(i) \left| T_g(i) - T_g^\circ \right|$$

where $\gamma(i)$ is defined in (4). Since choosing the penalization weight $\lambda \geq 0$ requires manual iteration, we consider the regulation problem as a hard constraint

$$q(k) \in R_3 \Rightarrow T_g(k) \in [T_g^\circ - \epsilon_T, T_g^\circ + \epsilon_T] \tag{8}$$

where $\epsilon_T$ is a small number relative to $T_g^\circ$ (e.g. $1\%$ of $T_g^\circ$).

*4) Generator speed:* Generator speed is also desired to lie between upper and lower bounds.

$$\omega_g^{lb} \leq \omega_g(k) \leq \omega_g^{ub} \tag{9}$$

In the case that these bounds do not exist, some non-constraining values can be used to improve the convergence rate of the optimization algorithm.

The generator speed should be regulated in the "high wind speed" region which is again enforced by hard constraints:

$$q(k) \in R_3 \Rightarrow \omega_g(k) \in [\omega_g^\circ - \epsilon_\omega, \omega_g^\circ + \epsilon_\omega] \tag{10}$$

*5) Blade pitch:* In the "low wind speed" region, the controller is not allowed to move the blades. Indeed, the blades pitch angles are constrained to the *maximum-lift angle*. As a result, the $\beta$-parameter that refers to the variation from the nominal blade pitch in region $R_2$ is constrained to

$$q(k) \in R_2 \Rightarrow \beta(k) = 0. \tag{11}$$

Moreover, the non–negativeness of blades pitch angle ($\beta$ here) and its upper bound is dictated by the mechanical fixtures

$$\beta^{lb} \leq \beta(k) \leq \beta^{ub}, \tag{12}$$

where $\beta^{lb}$ is zero in our case. Since an aggressive control law for changing the blade angles causes undesirable vibrations in the structure, the blade pitch rate is constrained by an upper bound chosen based on a fatigue analysis for the structure:

$$|\beta(k+1) - \beta(k)| \leq \delta_\beta \tag{13}$$

Here, $\delta_\beta = \dot{\beta}^{max} \times \tau$ where $\dot{\beta}^{max}$ is the maximum allowable blade pitch rate for the continuous system.

*6) Instantaneous power:* In high wind speed regime, $R_3$, both torque and speed will be regulated, and as a result, the instantaneous power will be also regulated. However, as long as the hybrid automaton is in mode $R_2$, the only constraints that can limit the power are the upper bounds on the torque and generator speed. As a result, if the product of these two terms is larger than the rated power in mode $R_3$, the controller will tend to stay in mode $R_2$. This may cause large values of instantaneous power – e.g. when $T_g^{ub}$ and $\omega_g^{ub}$ are large. Accordingly, we introduce an upper bound on the instantaneous power

$$P_k := T_g(k)\omega_g(k) \leq P^{max}. \tag{14}$$

Here, $P^{max}$ is based on the maximum safe operating power.

### C. Putting it all together

Assuming that $x(k)$ and $q(k)$ are known at each $k$ and the prediction of the wind speed is available for a horizon of $H$, our HMPC algorithm finds $\theta(k)$,

$$\theta(k) := \{\beta(k), \cdots, \beta(k+H-1), \\ T_g(k), \cdots, T_g(k+H-1), V_s\}$$

by solving the following optimization problem at each time step $k$.

$$\theta^*(k) = \arg\max_{\theta(k)} \sum_{i=k}^{k+H-2} T_g(i)\omega_g(i) - \lambda_1 \sum_{i=k}^{k+H-1} |p_i| \\ - \lambda_2 \sum_{i=k}^{k+H-2} |\gamma(i+1) - \gamma(i)| \tag{15a}$$

subject to:

$$x(j+1) = Ax(j) + B_w w(j) + B_\beta \beta(j) + B_T T_g(i) \tag{15b}$$
$$\omega_g(i) = Cx(i) \tag{15c}$$
$$q(i) \in \{R_2, R_3\} \tag{15d}$$
$$q(i) = R_3 \Leftrightarrow V(i) \geq V_s^k \tag{15e}$$
$$T_g^{lb} \leq T_g(i) \leq T_g^{ub} \tag{15f}$$
$$|T_g(j+1) - T_g(j)| \leq \delta_{T_g} \tag{15g}$$
$$q(i) = R_3 \Rightarrow T_g(i) \in [T_g^\circ - \epsilon_T, T_g^\circ + \epsilon_T] \tag{15h}$$
$$\omega_g^{lb} \leq \omega_g(i) \leq \omega_g^{ub} \tag{15i}$$
$$q(i) = R_3 \Rightarrow \omega_g(i) \in [\omega_g^\circ - \epsilon_\omega, \omega_g^\circ + \epsilon_\omega] \tag{15j}$$
$$q(i) = R_2 \Rightarrow \beta(i) = 0 \tag{15k}$$
$$\beta^{lb} \leq \beta(i) \leq \beta^{ub} \tag{15l}$$
$$|\beta(j+1) - \beta(j)| \leq \delta_\beta \tag{15m}$$
$$P_i := T_g(i)\omega_g(i) \leq P^{max} \tag{15n}$$

where $k \leq j \leq k+H-2$ and $k \leq i \leq k+H-1$. Once the optimization problem is solved at time step $k$, the optimal control signals $\beta^*(k) = \theta_1^*(k)$ and $T_g^*(k) = \theta_{H+1}^*(k)$ will be applied to the system – $\theta_i^*(k)$ refers to the $i$-th element of $\theta^*(k)$. An important point is that these two optimal values will be used as $\beta(k+1)$ and $T_g(k+1)$ for the two constraints (15m) and (15g) respectively.

## V. Results

In our simulation study, we have chosen a wind speed profile (Fig. 3) such that it contains both low and high wind speed operating regions of the wind turbine, and added white noise to model the prediction uncertainty. The time step in our simulation is $0.5s$ and the MPC horizon is 20 steps. Other parameters are given in Table I. We consider three cases analogous to the value functions introduced in section IV-A.

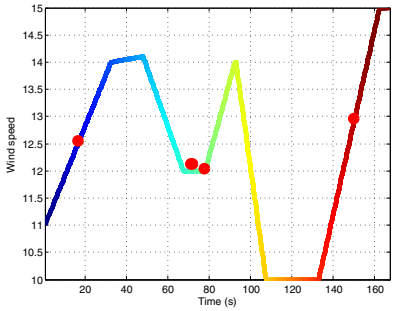


Fig. 3: Wind speed profile. The optimal switching wind speeds and moments are indicated by the circles. (Case 1)

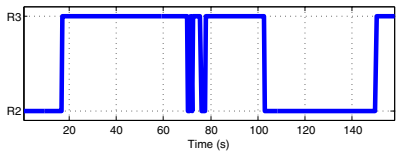


Fig. 4: Discrete modes of the system (Case 1).

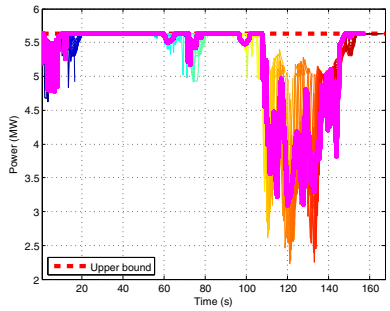


Fig. 5: Generator electric power (Case 1)

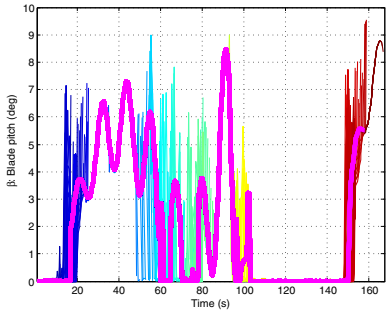


Fig. 6: Blade pitch angle (Case 1)

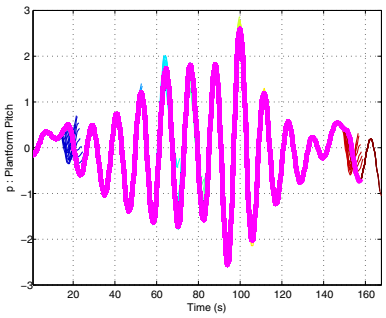


Fig. 7: Platform pitch angle (Case 1)

TABLE I: MPC Parameters

| | | | |
|---|---|---|---|
| $\tau$ | $0.5s$ | $H$ | 20 |
| $T_g^{ub}$ | $47.4\ KN$ | $T_g^{lb}$ | $20.0\ KN$ |
| $\omega_g^{ub}$ | $1250\ RPM$ | $\omega_g^{lb}$ | $1000\ RPM$ |
| $T_g^{max}$ | $15.0\ KN/s$ | $\delta\beta$ | $1^\circ$ |
| $P^{max}$ | $5.63\ MW$ | $\lambda_1, \lambda_2$ | 0 |

### *A. Case 1: No penalty for non-zero platform pitch angle and switching occurrences (i.e. $\lambda_1 = \lambda_2 = 0$)*

The optimal switching wind speeds in case 1 when the system transitions from region $R_2$ to region $R_3$ are indicated by red circles in Fig. 3 (the two circles at $71s$ and $72s$ cannot be distinguished in the figure). The corresponding modes of the system are depicted in Fig. 4, which shows that switching has occurred nine times. There are six transitions between $71s$ and $78s$ which is undesirable from a structural point of view. The purple line in Fig. 5 indicates turbine's captured power at different times. The other lines in the figure are the predicted trajectory of MPC in every time step. Since at each time step only the first control input is applied, these trajectories are not followed by the system. It can be seen from the figure that the results conform with the control objectives because power is regulated around the rated value whenever the system is in mode $R3$, and power capture is tried to be maximized when the system is in mode $R2$.

The platform pitch angle is shown in Fig. 7. As can be seen, the angle exceeds $2.5^\circ$ in this case which is a result of having no penalty on non-zero platform pitch angle. In summary, the drawbacks of the current value function are the large number of switching in a short period of time and large platform pitch angle. These results are summarized in Table II, where $P^{avg}$, $\sigma^p$ and $N^s$ denote the average power, standard deviation of the platform pitch angle and total number of switching occurrences respectively.

### *B. Case 2: Penalty for non-zero platform pitch angle ($\lambda_1 > 0, \lambda_2 = 0$)*

We have also considered a penalized value function as discussed in section IV-A to take the platform pitch into account. The simulation parameters are exactly the same as Table I except for $\lambda_1$ which is $5 \times 10^8$ in this new case. Figure 8 illustrates the compensated platform pitch angle which is considerably reduced after penalizing the value function. However, as is shown in Fig. 9 the switching occurrences have increased to 24 times which is undesirable. The average power for this case is given in Table II. These results show that penalization for the platform pitch angle has caused $4\%$ reduction in the average power.

### *C. Case 3: Penalty for non-zero platform pitch angle and switching occurrences ($\lambda_1 > 0, \lambda_2 > 0$):*

The final studied case corresponds to a value function that considers a mixture of power, platform pitch angle and number of switching. The performance of this scenario is given in Table II and the history of discrete states is

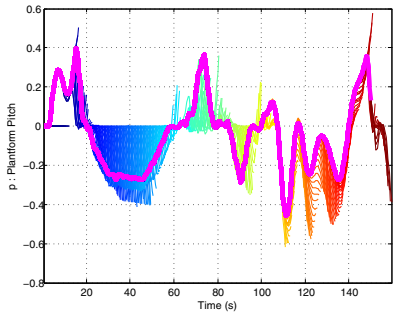


Fig. 8: Platform pitch angle (Case 2)

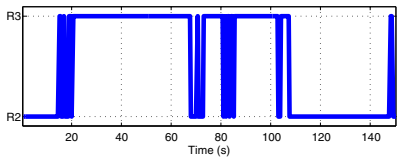


Fig. 9: Discrete modes of the system (Case 2)

TABLE II: Performance comparison between different value functions

| Case | Value function | $P^{avg}(MW)$ | $\sigma^p(\text{deg})$ | $N^s$ |
|---|---|---|---|---|
| 1 | $\lambda_1 = 0, \lambda_2 = 0$ | 5.23 | 0.94 | 9 |
| 2 | $\lambda_1 = 5_{\text{E}}8, \lambda_2 = 0$ | 5.15 | 0.18 | 24 |
| 3 | $\lambda_1 = 5_{\text{E}}8, \lambda_2 = 5_{\text{E}}7$ | 5.15 | 0.21 | 3 |

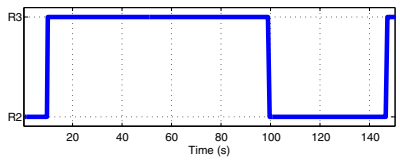


Fig. 10: Discrete modes of the system (Case 3)

shown in Fig. 10. These results show that the significant improvement in terms of platform pitch movement reduction and reduction in the number of switching is achieved at the cost of losing $4\%$ of the average power. The trade-off between these improvements and loss of the average power can be adjusted by using different values of $\lambda_1$ and $\lambda_2$.

## VI. Conclusion

The problem of designing a switching controller as well as finding the optimal switching point between low and high wind speed operating modes was addressed in this paper. The design was based on maximizing of power capture as well as minimization of platform pitch movement and number of switching. The problem was formalized using a hybrid MPC approach by considering all of the constraints in the low and high wind speed operating modes and also actuator limitations. Our simulation results indicate that penalizing both the blade pitch angle and the number of switching occurrences results in a control strategy that can avoid frequent mode transitions and keep the blade actuation low while the reduction in captured power is also small.

## References


[1] L. Y. Pao and K. E. Johnson, "Control of wind turbines," *Control Systems, IEEE*, vol. 31, no. 2, pp. 44–62, 2011.

[2] J. M. Jonkman, *Dynamics modeling and loads analysis of an offshore floating wind turbine*. ProQuest, 2007.

[3] O. Bagherieh, "Gain-scheduling control of floating offshore wind turbines on barge platforms," *Electronic Theses and Dissertations (ETDs) 2008+*, 2013.

[4] O. Bagherieh and R. Nagamune, "Gain-scheduling control of a floating offshore wind turbine above rated wind speed," *Control Theory and Technology*, vol. 13, no. 2, pp. 160–172, 2015.

[5] O. Bagherieh and R. Nagamune, "Utilization of blade pitch control in low wind speed for floating offshore wind turbines," in *American Control Conference (ACC), 2014*, pp. 4354–4359, IEEE, 2014.

[6] O. Bagherieh, K. Hedrick, and R. Horowitz, "Nonlinear control of floating offshore wind turbines using input/output feedback linearization and sliding control," in *ASME 2014 Dynamic Systems and Control Conference*, pp. V002T18A004–V002T18A004, American Society of Mechanical Engineers, 2014.

[7] G. van der Veen, I. Couchman, and R. Bowyer, "Control of floating wind turbines," in *American Control Conference (ACC), 2012*, pp. 3148–3153, IEEE, 2012.

[8] A. Wright and L. Fingersh, "Advanced control design for wind turbines," tech. rep., Technical Report NREL/TP-500-42437, 2008.

[9] E. Lindeberg, "Optimal control of floating offshore wind turbines," 2009.

[10] E. Camponogara, D. Jia, B. H. Krogh, and S. Talukdar, "Distributed model predictive control," *Control Systems, IEEE*, vol. 22, no. 1, pp. 44–52, 2002.

[11] B. Shahsavari, M. Maasoumy, A. Sangiovanni-Vincentelli, and R. Horowitz, "Stochastic model predictive control design for load management system of aircraft electrical power distribution," in *American Control Conference (ACC), 2015*, pp. 3649–3655, IEEE, 2015.

[12] A. Kusiak, Z. Song, and H. Zheng, "Anticipatory control of wind turbines with data-driven predictive models," *Energy Conversion, IEEE Transactions on*, vol. 24, no. 3, pp. 766–774, 2009.

[13] P. Moriarty and C. Butterfield, "Wind turbine modeling overview for control engineers," in *Proc. American Control Conf*, pp. 2090–2095, 2009.

[14] J. M. Jonkman and M. L. Buhl Jr, "Fast users guide," *Golden, CO: National Renewable Energy Laboratory*, 2005.

[15] A. Kumar and K. Stol, "Scheduled model predictive control of a wind turbine," in *Proceedings of AIAA/ASME Wind Energy Symposium*, 2009.

[16] M. Khalid and A. Savkin, "A model predictive control approach to the problem of wind power smoothing with controlled battery storage," *Renewable Energy*, vol. 35, no. 7, pp. 1520–1526, 2010.

[17] D. Schlipf, D. J. Schlipf, and M. Kühn, "Nonlinear model predictive control of wind turbines using lidar," *Wind Energy*, vol. 16, no. 7, pp. 1107–1129, 2013.

[18] D. Schlipf, D. J. Schlipf, and M. Kühn, "Nonlinear model predictive control of wind turbines using lidar," *Wind Energy*, vol. 16, no. 7, pp. 1107–1129, 2013.

[19] D. Dang, S. Wu, Y. Wang, and W. Cai, "Model predictive control for maximum power capture of variable speed wind turbines," in *IPEC, 2010 Conference Proceedings*, pp. 274–279, IEEE, 2010.

[20] A. Körber and R. King, "Model predictive control for wind turbines," in *European Wind Energy Conference*, 2010.

[21] L. C. Henriksen, *Model predictive control of a wind turbine*. PhD thesis, Technical University of Denmark, DTU, DK-2800 Kgs. Lyngby, Denmark, 2007.